Band structure of coupled InAs/GaSb quantum wells

S. de-Leon, L. D. Shvartsman, and B. Laikhtman
Racah Institute of Physics, The Hebrew University, Jerusalem 91904, Israel
(Received 11 March 1998; revised manuscript received 3 December 1998)

We calculate here the energy spectrum of InAs/GaSb heterostructure taking into account a complicated, anisotropic, and nonparabolic structure of the valence band of GaSb. In InAs/GaSb heterostructures the valence band of the GaSb layer overlaps with the conduction band of the InAs layer. The electrons in the InAs layer are coupled to the holes in the GaSb layer and a hybridization gap is formed. The coupling is considered here as a small perturbation for the problem of two decoupled infinite quantum wells, one of holes and one of electrons. The band structure of the coupled system shows features that result from anisotropy, dependence of the coupling on the in-plane vector, and lifting of the double degeneracy of the energy bands of electrons and holes due to the coupling. The splitting of the energy bands is very important at the crossing point. Interesting results of these effects are the possibility of a new kind of a gapless state and nontrivial constant energy contours. [S0163-1829(99)02027-5]

I. INTRODUCTION

The unique features of InAs/GaSb heterostructures increase the interest in investigating these systems. The lattice constants of the two materials are very close, and therefore matching of thin layers of these materials is possible. The experimental results for these heterostructures reveal magnetic and electronic features that deviate substantially from well known features of other kinds of quantum wells and make these systems both very promising for device application and intriguing from the fundamental point of view. For example, InAs/GaSb structure is the most perspective candidate for the observation of Bose-Einstein condensation of excitons.[1–10]

In some range of the layers widths, the bottom of the first conduction sub-band in the InAs layer lays below the top edge of the first valence sub-band in the GaSb layer. This overlap between the valence band in GaSb and the conduction band in InAs means that from either side of the interface there are allowed states that differ from each other in the total angular momentum and in the sign of the effective mass. Electron wave functions in InAs layer are superpositions of s states, and their total angular momentum is $J=1/2$. Hole wave functions are superposition of p states, and their total angular momentum is $J=3/2$.

The overlap between the valence band in GaSb and the conduction band in InAs induces charge transfer from GaSb to InAs and the ground state of this system is spatially separated two-dimensional electrons gas (2DEG) in the InAs layer and two-dimensional holes gas (2DHG) in the GaSb layer. The tunneling between the GaSb and InAs layers yields the formation of a gap in the energy spectrum. This gap comes about at the crossing point of the GaSb and InAs separate spectra and it can be controlled by an external electric field.[11,12] This hybridization gap has been recently observed experimentally in double thin layers of InAs/GaSb[13–15] and in superlattices.[16]

In cyclotron resonance (CR) experiments in this system additional absorption lines were measured.[17–20] A large number of observed CR peaks contradicts to intuitive understanding in which only two lines are expected, one for electrons and one for holes. For an understanding of these results we have to perform an accurate calculation of the band structure of the system. This is the purpose of the present paper.

The problem is not trivial because even the bulk valence band in GaSb has a complicated structure—there are two highly anisotropic sub-bands.[21] Since we are dealing with thin layers of InAs/GaSb we need to consider the size quantization mixing heavy and light hole sub-bands and resulting in a highly nonparabolic spectrum.[22–27] The incorporation of the ground electron sub-band of InAs makes the problem even more complicated. In previous calculations[28–34] these features were not explicitly investigated.

In this paper we consider the exact structure of the holes spectrum, and use the perturbation theory to derive the spectrum of a system of thin double layers of InAs and GaSb sandwiched between two high potential barriers. The unperturbed problem is the problem of two decoupled infinite quantum wells, one of electrons and one of holes. The perturbation is the coupling between the wells induced by the tunneling between the layers.

For solving the unperturbed decoupled problem we use the envelope function approximation where hole states are four-component spinors and electron states are two-component spinors. For the calculation the boundary conditions at the interface between the InAs layer and the GaSb layer are required. The crucial point here is the necessity to match states with different number of components that correspond to different total electron and hole angular momenta. We have used a variation principle to derive phenomenological boundary conditions that do not depend on any microscopical model. This method is described in our earlier paper.[35]

One more important factor here is the self-consistent potential induced by the charge transfer. From the results of simpler models[12,36] we see that the main effect of this potential is a constant shift of the bands which decreases the overlap. The spectrum curvature is almost unaffected. Therefore in the present paper we present both the spectrum calculated without self-consistent potential corrections and with them.

 ©1999 The American Physical Society

For the calculation of these corrections we use the simple model that is described in our previous paper.[36]

The results show that when the overlap between the holes and the electrons is large enough the system can reach a stage where the anisotropy effects the position of the InAs and GaSb spectra crossing point. With the change of the in-plane wave vector **k** direction the energy position of the crossing point changes. In such a case there is a hybridization gap in every direction of **k** but the energy position of the gap is angular dependent. If the anisotropy is so substantial that the difference between the energy position of the gap in different directions (ΔE_g), is larger than the gap itself (i.e., $\Delta E_g > E_g$) then the density of states is actually gapless and the system exhibits a kind of a semimetal phase.

Another aspect of the exact calculation is a complete lifting of the degeneracy in the energy spectrum. Both ground sub-bands of holes and electrons in the decoupled unperturbed problem are doubly degenerated (Kramers degeneracy). The coupling between the bands lifts the degeneracy and a small splitting in the energy spectrum occurs. This splitting is negligible in most of the spectrum range except the crossing point where it is the key factor determining the gap size. Both the gap size and the position of the crossing point depend on the well width. All these effects yield nontrivial constant energy contours that change substantially with the energy.

In the next section we develop the perturbation theory for this problem. In the third section we use symmetry considerations and some physical assumptions to simplify the results and present the final results of the calculations, i.e., the dependence of the coupling strength on the in-plane vector, the energy spectrum of the system in different in-plane angles, and some constant energy contours. The notations that we used for the general form of the solution are given in the Appendix.

II. THE PROBLEM AND EQUATIONS

The structure that we investigate here consists of two thin layers, one of InAs and one of GaSb. The geometry of the system is the following: to the left,

$$-L_c-\frac{L_v}{2}<z<-\frac{L_v}{2},$$

there is an InAs layer which is a quantum well for electrons. To the right,

$$-\frac{L_v}{2}<z<\frac{L_v}{2},$$

there is a GaSb layer which is a quantum well for holes. The two layers are sandwiched between high potential barriers, and we assume that the wave function vanishes at these barriers. We use this assumption for simplification. The method can be applied also for the problem of two finite quantum wells of holes and of electrons, but the calculation is much more cumbersome.

We use the envelope function approximation for our calculations. The system of equations includes Schrödinger equations for hole and electron envelope functions and boundary conditions at the interface between the layers.

The Schrödinger equations are

$$\mathcal{H}_e\psi_e=E\psi_e, \quad -L_c-\frac{L_v}{2}<z<-\frac{L_v}{2}, \tag{2.1a}$$

$$\mathcal{H}_h\psi_h=E\psi_h, \quad -\frac{L_v}{2}<z<\frac{L_v}{2}. \tag{2.1b}$$

Here ψ_e is two-component electron wave function, ψ_h is the four-component hole wave function

$$\mathcal{H}_e=-\frac{\hbar^2}{2m_e}\nabla^2, \tag{2.2a}$$

$$\mathcal{H}_h=\Delta+\frac{\hbar^2}{2m_0}\left[\left(\gamma_1+\frac{5}{2}\gamma_2\right)\nabla^2-2\gamma_3(\vec{J}\vec{\nabla})^2+2(\gamma_3-\gamma_2)\left(\frac{\partial^2}{\partial x^2}J_x^2+\frac{\partial^2}{\partial y^2}J_y^2+\frac{\partial^2}{\partial z^2}J_z^2\right)\right]. \tag{2.2b}$$

Here $\mathcal{H}_h$ is the Luttinger effective Hamiltonian for GaSb.[21] $\vec{J}$ is the total angular momentum vector operator corresponding to the angular momentum 3/2, and $\gamma_1=11.8$, $\gamma_2=4.03$, $\gamma_3=5.26$ are the Luttinger parameters for GaSb.[37] J_x, J_y, and J_z are 4×4 matrices, i.e., we treat properly both the degeneracy of light and heavy holes and the warping of the valence band isoenergetic surfaces. $\Delta\approx150$ meV is the energy difference between the bottom of the conduction band in bulk InAs and the top of the valence band in bulk GaSb. m_e is the effective mass of the conduction electrons in InAs. The boundary conditions at the interface between the two layers $z=-L_v/2$ were derived in our previous work:[35]

$$\mathcal{A}_e\psi_e+\mathcal{B}^\dagger\psi_h=\mathcal{D}_e\psi_e, \tag{2.3a}$$

$$\mathcal{A}_h\psi_h+\mathcal{B}\psi_e=\mathcal{D}_h\psi_h, \tag{2.3b}$$

where the differential operators $\mathcal{D}_e$, $\mathcal{D}_h$ are

$$\mathcal{D}_e=-\frac{\hbar^2}{2m_e}\frac{\partial}{\partial z}, \tag{2.4a}$$

$$\mathcal{D}_h=-\frac{\hbar^2}{2m_0}\left[\left(\gamma_1+\frac{5}{2}\gamma_2-2\gamma_2J_z^2\right)\frac{\partial}{\partial z}-\gamma_3(J_z\vec{J}_\parallel+\vec{J}_\parallel J_z)\vec{\nabla}_\parallel\psi_h\right]. \tag{2.4b}$$

Here we use the following notations for the in-plane vectors: $\vec{J}_\parallel=(J_x,J_y)$, $\vec{\nabla}_\parallel=(\partial/\partial x,\partial/\partial y)$. In Eq. (2.3) $\mathcal{A}_e$ is 2×2 matrix that represents the interface energy of electrons states, $\mathcal{A}_h$ is a 4×4 matrix which represents the interface energy of holes states. $\mathcal{B}$ is a 4×2 matrix which represents the tunneling between the layers. The units of the matrix elements are $[E\times L]$—energy multiplied by length. Since the scales of the interface region are microscopic, we can say that, in general, the matrix elements are of the order of $\hbar^2/2\sqrt{m_em_h}a$, where m_e, m_h are the effective masses of electrons and holes, respectively, and a is the lattice constant. It can be shown from symmetry consideration that both $\mathcal{A}_e$ and $\mathcal{A}_h$ are diagonal in the representation where J_z is diagonal. The same argument shows that the only nonvan-

ishing matrix elements of $\mathcal{B}$ are $\mathcal{B}_{21}$, $\mathcal{B}_{32}$. (More precisely, the interface has a lower symmetry than the crystal itself. Nevertheless, we considered the anisotropy that results from this lower symmetry to be small, and neglected it.[38]) More details about the above estimations and symmetry arguments are presented in Ref. 35.

With a little algebra we can derive from Eq. (2.3) a more convenient form of the boundary conditions

$$\psi_e = \mathcal{M}_{ee}\psi_e + \mathcal{M}_{eh}\psi_h , \tag{2.5a}$$

$$\psi_h = \mathcal{M}_{he}\psi_e + \mathcal{M}_{hh}\psi_h . \tag{2.5b}$$

Here $\mathcal{M}_{ee}, \mathcal{M}_{eh}, \mathcal{M}_{he}, \mathcal{M}_{hh}$, are the differential operators

$$\mathcal{M}_{ee} = (\mathcal{A}_e - \mathcal{B}^\dagger \mathcal{A}_h^{-1}\mathcal{B})^{-1}\mathcal{D}_e , \tag{2.6a}$$

$$\mathcal{M}_{eh} = -(\mathcal{A}_e - \mathcal{B}^\dagger \mathcal{A}_h^{-1}\mathcal{B})^{-1}\mathcal{B}^\dagger \mathcal{A}_h^{-1}\mathcal{D}_h , \tag{2.6b}$$

$$\mathcal{M}_{he} = -(\mathcal{A}_h - \mathcal{B}\mathcal{A}_e^{-1}\mathcal{B}^\dagger)^{-1}\mathcal{B}\mathcal{A}_e^{-1}\mathcal{D}_e , \tag{2.6c}$$

$$\mathcal{M}_{hh} = (\mathcal{A}_h - \mathcal{B}\mathcal{A}_e^{-1}\mathcal{B}^\dagger)^{-1}\mathcal{D}_h . \tag{2.6d}$$

The dispersion relation that we are going to obtain making use of Eq. (2.1) with boundary conditions (2.5) is the dependence of the energy on the in-plane wave vector $\mathbf{k}$. So hereafter we assume that wave function dependence on x and y is determined by the exponential factor $e^{i\mathbf{k}\mathbf{r}_\parallel}$. Then the differential operators $\partial/\partial x$ and $\partial/\partial y$ in Eqs. (2.1) and (2.5) are replaced by ik_x and ik_y respectively, and the only derivatives that remain in these equations are with respect to z.

The right-hand sides of Eqs. (2.5) are of the order of $\mathcal{D}\mathcal{A}^{-1}$ [see Eq. (2.6)]. As was mentioned above, $\mathcal{A}^{-1}$ is proportional to the lattice constant a while the differential operator $\mathcal{D}$ operating on wave functions is proportional to the macroscopic scale $1/L$ where L is the wells widths. This means that the product $\mathcal{D}\mathcal{A}^{-1}$ is proportional to the small ratio a/L. We are going to develop a perturbation theory in this parameter. The same parameter justifies the envelope function approximation, so our method is consistent.

If terms of the order of a/L are neglected the boundary conditions at the interface between the layers, Eq. (2.5), are reduced to $\psi_e = \psi_h = 0$ at $z = -L_v/2$. This corresponds to two decoupled quantum wells, one of electrons and one of holes. In our method we use this decoupled problem as an unperturbed system. This system is solvable, and we will derive the spectrum of the coupled problem perturbing the solution of the decoupled problem.

For electrons the dispersion relation of the unperturbed problem is parabolic and isotropic. For holes the dispersion relation is anisotropic and nonparabolic in the in-plane k vector.

Under the assumption of weak coupling we can write the perturbed wave function as a linear combination of the unperturbed wave functions and the coupling determines the coefficients in this linear combination. We assume that only the ground sub-band of each well is occupied and we are interested in the new ground sub-band of the system. The ground sub-band of the unperturbed problem for electrons is doubly degenerate due to spin. The ground sub-band of the unperturbed holes is also doubly degenerate.[26] The hole degeneracy is related to the reflection with respect to the layer plane. This symmetry is broken in the coupled system, and we expect that this would lift the degeneracy of the ground sub-band. We express the coupled ground state in a combination of the degenerate ground states and the contribution from the higher levels in the decoupled problem

$$\psi_e = v_\uparrow \psi^{(0)}_{e,\uparrow} + v_\downarrow \psi^{(0)}_{e,\downarrow} + \sum_n v_{en}\psi^{(0)}_{en} , \tag{2.7a}$$

$$\psi_h = u_{\mathrm{even}}\psi^{(0)}_{h,\mathrm{even}} + u_{\mathrm{odd}}\psi^{(0)}_{h,\mathrm{odd}} + \sum_n u_{hn}\psi^{(0)}_{hn} . \tag{2.7b}$$

Here the amplitudes are defined as

$$v_\uparrow = \langle \psi^{(0)}_{e,\uparrow} | \psi_e \rangle, \quad v_\downarrow = \langle \psi^{(0)}_{e,\downarrow} | \psi_e \rangle, \tag{2.8a}$$

$$u_{\mathrm{even}} = \langle \psi^{(0)}_{h,\mathrm{even}} | \psi_h \rangle, \quad u_{\mathrm{odd}} = \langle \psi^{(0)}_{h,\mathrm{odd}} | \psi_h \rangle. \tag{2.8b}$$

Angular brackets here denote the integration with respect to z. The wave functions of the higher levels are orthogonal to the ground state wave functions. In our representation the holes wave functions are four-components spinors and the electrons wave functions are two-component spinors. The explicit form of the ground state wave functions for infinite well of holes are well known but very cumbersome,[27] so we do not present them here. The explicit form of the ground state wave function for the electron infinite well in our representation is

$$\psi^{(0)}_{e,\uparrow} = \begin{pmatrix} \tilde{\psi}_{e\uparrow}(z) \\ 0 \end{pmatrix} e^{i\mathbf{k}\cdot\mathbf{r}}, \quad \psi^{(0)}_{e,\downarrow} = \begin{pmatrix} 0 \\ \tilde{\psi}_{e\downarrow}(z) \end{pmatrix} e^{i\mathbf{k}\cdot\mathbf{r}}, \tag{2.9}$$

where

$$\tilde{\psi}_{e\uparrow}(z) = \tilde{\psi}_{e\downarrow}(z) = \sqrt{\frac{2}{L_c}} \sin \frac{\pi}{L_c}\left(z + \frac{L_v}{2} \right). \tag{2.10}$$

Now we will derive equations for the amplitudes $v_\uparrow, v_\downarrow, u_{\mathrm{even}}, u_{\mathrm{odd}}$. From these equations we will derive the dispersion relation of the ground state of the coupled problem. To obtain the required equations we multiply Eqs. (2.1a) and (2.1b) by the ground states wave function of the unperturbed problem and integrate with respect to the z over the relevant well region. The equations are

$$0 = \langle \psi^{(0)}_{e,\uparrow} | \mathcal{H}_e - E | \psi_e \rangle, \tag{2.11a}$$

$$0 = \langle \psi^{(0)}_{e,\downarrow} | \mathcal{H}_e - E | \psi_e \rangle, \tag{2.11b}$$

$$0 = \langle \psi^{(0)}_{h,\mathrm{even}} | \mathcal{H}_h - E | \psi_h \rangle, \tag{2.11c}$$

$$0 = \langle \psi^{(0)}_{h,\mathrm{odd}} | \mathcal{H}_h - E | \psi_h \rangle. \tag{2.11d}$$

Calculating the terms in these equations that do not contain derivatives with respect to z we use the definitions of the amplitudes, Eq. (2.8). Terms containing the derivatives we integrate by parts in order to reduce them to the form where the derivatives operate only on unperturbed wave functions. Then we can make use of the Schrödinger equations for the unperturbed wave functions. In the integration by parts we obtain also integrated terms from the interface between InAs and GaSb wells (integrated terms from other interfaces are

zero due to zero boundary conditions for the wave functions). As a result we obtain the following equations:

$$0=v_{\uparrow}[E_e^{(0)}(\vec{k})-E]+\frac{\hbar^2}{2m_e}\frac{\partial\psi_{e,\uparrow}^{\dagger(0)}}{\partial z}\psi_e\Big|_{z=-L_v/2}, \quad (2.12a)$$

$$0=v_{\downarrow}[E_e^{(0)}(\vec{k})-E]+\frac{\hbar^2}{2m_e}\frac{\partial\psi_{e,\downarrow}^{\dagger(0)}}{\partial z}\psi_e\Big|_{z=-L_v/2}, \quad (2.12b)$$

$$0=u_{\rm even}[E_h^{(0)}(\vec{k})-E]+\frac{\hbar^2}{2m_0}\frac{\partial\psi_{h,\rm even}^{\dagger(0)}}{\partial z}\times\left(\gamma_1+\frac{5}{2}\gamma_2-2\gamma_2 J_z^2\right)\psi_h\Big|_{z=-L_v/2}, \quad (2.12c)$$

$$0=u_{\rm odd}[E_h^{(0)}(\vec{k})-E]+\frac{\hbar^2}{2m_0}\frac{\partial\psi_{h,\rm odd}^{\dagger(0)}}{\partial z}\times\left(\gamma_1+\frac{5}{2}\gamma_2-2\gamma_2 J_z^2\right)\psi_h\Big|_{z=-L_v/2}, \quad (2.12d)$$

where $E_e^{(0)}(\vec{k})$ and $E_h^{(0)}(\vec{k})$ are the unperturbed dispersion relations for electrons, and holes, respectively.

For the wave functions at the interface between the layers, $z=-L_v/2$, in Eq. (2.12) we use their expressions from the boundary conditions, Eqs. (2.5). As it was mentioned above the right-hand side of the boundary conditions contains the small parameter a/L. Neglecting high order terms in a/L we can replace wave functions there with their unperturbed values and neglect the contribution of the high levels. Then with the help of Eq. (2.7) the expressions for wave functions at the interface are

$$\psi_e=\mathcal{M}_{ee}(v_{\uparrow}\psi_{e,\uparrow}^{(0)}+v_{\downarrow}\psi_{e,\downarrow}^{(0)})+\mathcal{M}_{eh}(u_{\rm even}\psi_{h,\rm even}^{(0)}+u_{\rm odd}\psi_{h,\rm odd}^{(0)}), \quad (2.13a)$$

$$\psi_h=\mathcal{M}_{he}(v_{\uparrow}\psi_{e,\uparrow}^{(0)}+v_{\downarrow}\psi_{e,\downarrow}^{(0)})+\mathcal{M}_{hh}(u_{\rm even}\psi_{h,\rm even}^{(0)}+u_{\rm odd}\psi_{h,\rm odd}^{(0)}). \quad (2.13b)$$

The substitution of these expressions in the interface terms in Eq. (2.12) leads to four equations for the four amplitudes $u_{\rm even}$, $u_{\rm odd}$, $v_{\uparrow}$, and $v_{\downarrow}$ where all coefficients except the energy E are known. This set of equations has a nontrivial solution, only if its determinant equals to zero. The condition for the vanishing of the determinant, provides us with the desired dispersion relation of the coupled problem. The explicit general form of the determinant is

$$\begin{vmatrix}
E_e^{(0)}-E-C_{\uparrow}\left|\frac{\partial\tilde{\psi}_{e,\uparrow}^{(0)}}{\partial z}\right|^2 & 0 & C_{21}^{*}\frac{\partial\tilde{\psi}_{e,\uparrow}^{(0)}}{\partial z}\frac{\partial\tilde{\psi}_{h,\rm odd,1/2}^{(0)}}{\partial z} & C_{21}^{*}\frac{\partial\tilde{\psi}_{e,\uparrow}^{(0)}}{\partial z}\frac{\partial\tilde{\psi}_{h,\rm even,1/2}^{(0)}}{\partial z} \\
0 & E_e^{(0)}-E-C_{\downarrow}\left|\frac{\partial\tilde{\psi}_{e,\downarrow}^{(0)}}{\partial z}\right|^2 & C_{32}^{*}\frac{\partial\tilde{\psi}_{e,\downarrow}^{(0)}}{\partial z}\frac{\partial\tilde{\psi}_{h,\rm odd,-1/2}^{(0)}}{\partial z} & C_{32}^{*}\frac{\partial\tilde{\psi}_{e,\uparrow}^{(0)}}{\partial z}\frac{\partial\tilde{\psi}_{h,\rm even,-1/2}^{(0)}}{\partial z} \\
C_{21}\frac{\partial\tilde{\psi}_{e,\uparrow}^{(0)}}{\partial z}\frac{\partial\tilde{\psi}_{h,\rm odd,1/2}^{*(0)}}{\partial z} & C_{32}\frac{\partial\tilde{\psi}_{e,\downarrow}^{(0)}}{\partial z}\frac{\partial\tilde{\psi}_{h,\rm odd,-1/2}^{*(0)}}{\partial z} & E_h^{(0)}-E-G\left(\left|\frac{\partial\psi_{h,\rm odd}^{(0)}}{\partial z}\right|^2\right) & F\left(\frac{\partial\psi_{h,\rm odd}^{*(0)}}{\partial z},\frac{\partial\psi_{h,\rm even}^{(0)}}{\partial z}\right) \\
C_{21}\frac{\partial\tilde{\psi}_{e,\uparrow}^{(0)}}{\partial z}\frac{\partial\tilde{\psi}_{h,\rm even,1/2}^{*(0)}}{\partial z} & C_{32}\frac{\partial\tilde{\psi}_{e,\downarrow}^{(0)}}{\partial z}\frac{\partial\tilde{\psi}_{h,\rm even,-1/2}^{*(0)}}{\partial z} & F\left(\frac{\partial\psi_{h,\rm even}^{*(0)}}{\partial z},\frac{\partial\psi_{h,\rm odd}^{(0)}}{\partial z}\right) & E_h^{(0)}-E-G\left(\left|\frac{\partial\psi_{h,\rm even}^{(0)}}{\partial z}\right|^2\right)
\end{vmatrix}. \quad (2.14)$$

Here we use the notation for the hole envelope function components from Ref. 27 where the expressions for these components are written down explicitly. Other notations are presented in the Appendix.

The off-diagonal terms between the odd and the even hole states appear due to the symmetry breaking with respect to the parity operator. The unperturbed system of holes was that of an infinite well. This system is symmetric with respect to the parity.[26] The perturbed system is not symmetric with respect to the reflection in xy plane and therefore the degeneracy with respect to the parity is lifted.

We see here that there are contributions of the perturbation to diagonal terms. The initial spectrum of holes and electrons is renormalized by the small perturbation. The additional diagonal terms are by the order of magnitude smaller than original unperturbed diagonal terms.

The off-diagonal terms between electrons and holes are the most relevant to the effect that we investigate here. The structure of these terms shows that only states with the same angular momentum are coupled.

In the next section we will use symmetry and other physical assumptions to reduce the general form of the determinant to a more convenient, solvable form. The final results of the calculation are presented for this simplified form.

III. LEGITIMATE APPROXIMATION

The general form of the determinant, Eq. (2.14), is very cumbersome and includes a lot of different parameters. However, symmetry considerations and other physical assumptions can be used to simplify the problem.

We assume that the surface energy is invariant with respect to the change of the sign of the total angular momentum projection to the z direction. That yields the following relations between the interface matrix elements:

$$\mathcal{A}_{h,11}=\mathcal{A}_{h,44}\equiv\mathcal{A}_{h,3/2}, \quad \mathcal{A}_{h,22}=\mathcal{A}_{h,33}\equiv\mathcal{A}_{h,1/2}, \quad (3.1a)$$

$$\mathcal{A}_{e,11}=\mathcal{A}_{e,22}\equiv\mathcal{A}_{e,1/2}, \quad \mathcal{B}_{21}=\mathcal{B}_{32}\equiv\mathcal{B}_{1/2}. \quad (3.1b)$$

This reduces the number of parameters in this problem to 4 complex coefficients.

The effect that we investigate here is the coupling between the electrons and the holes. We would like to concentrate on this and neglect other effects that results from the boundary conditions. As was mentioned above, additional diagonal terms that renormalize the unperturbed spectrum are by the order of magnitude smaller than the original unperturbed diagonal terms. Therefore we neglect them in the determinant. The breaking of parity symmetry induces off-diagonal terms between the odd and the even holes functions. We neglect this effect in order to simplify the determinant.

Under all the assumptions that were described above the number of parameters in the problem reduces to one complex coefficient

$$C=\frac{\hbar^2}{2m_0}\frac{\hbar^2}{2m_e}\frac{\mathcal{B}_{1/2}(\gamma_1+2\gamma_2)}{\mathcal{A}_{h,1/2}\mathcal{A}_{e,1/2}-|\mathcal{B}_{1/2}|^2}. \tag{3.2}$$

But as we will see the energy spectrum depends only on $|C|$, so actually there is just one real parameter in the problem.

As was mentioned in the previous section, the units of the interface matrix elements are energy multiplied by length and the scales are the atomic scales. So a good estimate for $|C|$ will be $\hbar^2 a/2\sqrt{m_e m_{lh}}$, where $m_{lh}=m_0/(\gamma_1+2\gamma_2)\approx 0.05m_0$ is the effective mass of GaSb light holes and $m_e=0.026m_0$ is the effective mass of InAs conduction electrons. The determinant now has the following form:

$$0=\begin{vmatrix} E_e^{(0)}-E & 0 & C^*\dfrac{\partial\tilde{\psi}_{e,\uparrow}^{(0)}}{\partial z}\dfrac{\partial\tilde{\psi}_{h,\mathrm{odd},1/2}^{(0)}}{\partial z} & C^*\dfrac{\partial\tilde{\psi}_{e,\uparrow}^{(0)}}{\partial z}\dfrac{\partial\tilde{\psi}_{h,\mathrm{even},1/2}^{(0)}}{\partial z} \\ 0 & E_e^{(0)}-E & C^*\dfrac{\partial\tilde{\psi}_{e,\downarrow}^{(0)}}{\partial z}\dfrac{\partial\tilde{\psi}_{h,\mathrm{odd},-1/2}^{(0)}}{\partial z} & C^*\dfrac{\partial\tilde{\psi}_{e,\downarrow}^{(0)}}{\partial z}\dfrac{\partial\tilde{\psi}_{h,\mathrm{even},-1/2}^{(0)}}{\partial z} \\ C\dfrac{\partial\tilde{\psi}_{e,\uparrow}^{(0)}}{\partial z}\dfrac{\partial\tilde{\psi}_{h,\mathrm{odd},1/2}^{*(0)}}{\partial z} & C\dfrac{\partial\tilde{\psi}_{e,\downarrow}^{(0)}}{\partial z}\dfrac{\partial\tilde{\psi}_{h,\mathrm{odd},-1/2}^{*(0)}}{\partial z} & E_h^{(0)}-E & 0 \\ C\dfrac{\partial\tilde{\psi}_{e,\uparrow}^{(0)}}{\partial z}\dfrac{\partial\tilde{\psi}_{h,\mathrm{even},1/2}^{*(0)}}{\partial z} & C\dfrac{\partial\tilde{\psi}_{e,\downarrow}^{(0)}}{\partial z}\dfrac{\partial\tilde{\psi}_{h,\mathrm{even},-1/2}^{*(0)}}{\partial z} & 0 & E_h^{(0)}-E \end{vmatrix}, \tag{3.3}$$

where

$$|C|\approx\frac{\hbar^2 a}{2\sqrt{m_e m_{lh}}}. \tag{3.4}$$

The values of the effective masses were given above and $a\approx 6$ Å.

This determinant is a polynomial of the fourth order in the energy which has four different roots. We begin the calculation of the spectrum with two degenerate sub-bands, one is the electron ground state in the InAs, and the other is the hole ground state in the GaSb. The degeneracy of the ground states is lifted due to the coupling between the energy bands. The effect of splitting of the energy bands due to coupling is negligible except the region near the crossing points.

The solutions to Eq. (3.3) can be written in the form

$$E_{1,2,3,4}=\frac{(E_e^{(0)}+E_h^{(0)})}{2}\pm\frac{1}{2}\sqrt{(E_e^{(0)}-E_h^{(0)})^2+4X_{1,2}}, \tag{3.5}$$

where

$$X_{1,2}=\frac{b}{2}\pm\frac{1}{2}\sqrt{b^2-4d}. \tag{3.6}$$

Here

$$b=|C|^2\left|\frac{\partial\tilde{\psi}_e}{\partial z}\right|^2\left(\left|\frac{\partial\tilde{\psi}_{h,\mathrm{odd},1/2}^{(0)}}{\partial z}\right|^2+\left|\frac{\partial\tilde{\psi}_{h,\mathrm{odd},-1/2}^{(0)}}{\partial z}\right|^2+\left|\frac{\partial\tilde{\psi}_{h,\mathrm{even},1/2}^{(0)}}{\partial z}\right|^2+\left|\frac{\partial\tilde{\psi}_{h,\mathrm{even},-1/2}^{(0)}}{\partial z}\right|^2\right), \tag{3.7a}$$

$$d=|C|^4\left|\frac{\partial\tilde{\psi}_e}{\partial z}\right|^4\left|\frac{\partial\tilde{\psi}_{h,\mathrm{odd},1/2}^{(0)}}{\partial z}\frac{\partial\tilde{\psi}_{h,\mathrm{even},-1/2}^{(0)}}{\partial z}-\frac{\partial\tilde{\psi}_{h,\mathrm{odd},-1/2}^{(0)}}{\partial z}\frac{\partial\tilde{\psi}_{h,\mathrm{even},1/2}^{(0)}}{\partial z}\right|^2. \tag{3.7b}$$

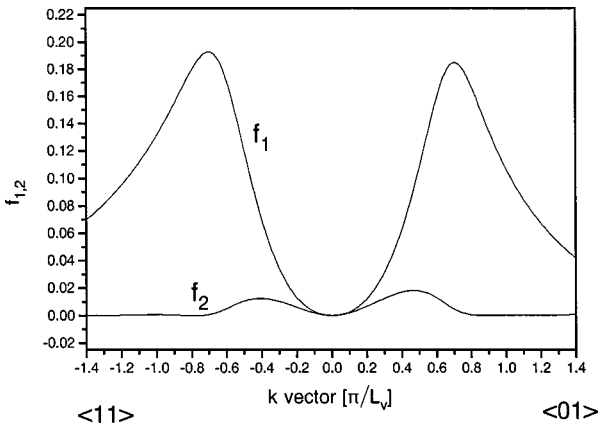

FIG. 1. The coupling dependence on the in-plane vector, in the in-plane directions ⟨01⟩ and ⟨11⟩.

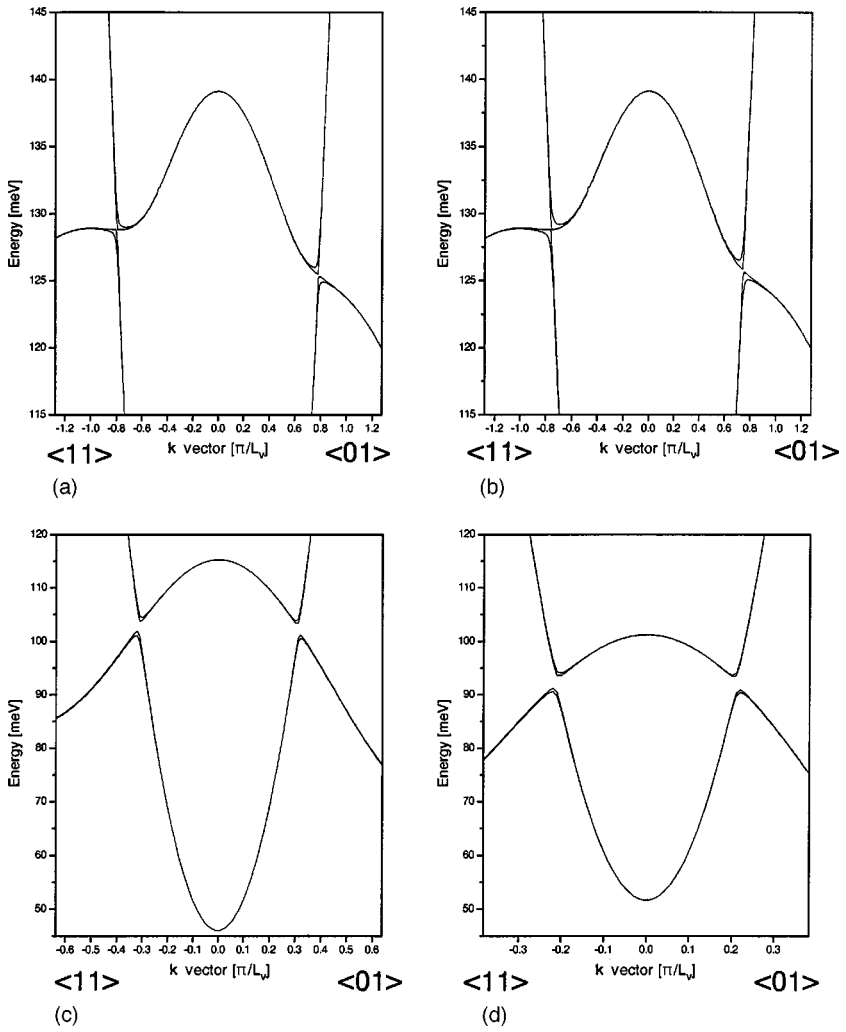

FIG. 2. The energy spectrum for different wells widths. The zero energy point is at the bottom of the bulk InAs conduction band. We considered the hole well of 0.4 eV depth and the electron well of 0.8 eV depth. (a) $L_v=100$ Å, $L_c=170$ Å, (b) $L_v=100$ Å, $L_c=150$ Å, (c) $L_v=50$ Å, $L_c=150$ Å, (d) $L_v=40$ Å, $L_c=140$ Å.

Here we used the notation $\partial\tilde{\psi}_e/\partial z \equiv \partial\tilde{\psi}^{(0)}_{e,\uparrow}/\partial z = \partial\tilde{\psi}^{(0)}_{e,\downarrow}/\partial z$ [Eq. (2.10)]. It is important to note that the hole spectrum $E_h^{(0)}$ in Eq. (3.5) is the ground heavy hole sub-band while the corrections in Eq. (3.7) are calculated with the light holes component of the holes wave function. This is indicated explicitly by the subscript $\pm 1/2$ which describes the angular momentum projection in the z direction.

The results of numerical calculation of the spectrum according to Eq. (3.5) are presented in the next section. The unperturbed energies $E_h^{(0)}$ and $E_e^{(0)}$ were found by the numerical solution of the problems for rectangular quantum wells similar to Ref. 26. For a better accuracy the unperturbed energy spectrum of holes and of electrons were calculated for finite wells of holes and electrons. In reality, the well of holes in GaSb is limited by finite barriers between the valence band top in GaSb and the tops of the valence bands in InAs and AlSb. The well for electrons is determined in a similar way. We neglected the asymmetry of the barriers. For holes this asymmetry is really small (0.42 eV and 0.51 eV for InAs and AlSb barriers, respectively) and for electrons the whole correction due to the finiteness of the well is very small.

In the development of the method in both the present section and Sec. II and the calculation of tunneling across the interface we used the approximation of infinite wells. This approximation can be justified in the following way. The corrections to the energies and the wave functions of electrons and holes due to the well finiteness are of the order of the square root of the ratio of the quantization energy in the well to the barrier height $\sqrt{\Delta E/U}$. Making use of the infinite well approximation we neglect corrections of this order to $X_{1,2}$ in Eq. (3.5). The quantities $X_{1,2}$ themselves are proportional to the small parameter a/L. So, in the spectrum we keep terms of the order of a/L and $\sqrt{\Delta E/U}$ and neglect terms containing the product of these two small parameters. It is worth to note that the neglect of corrections of the order of $\sqrt{\Delta E/U}$ to wave functions is justified for $X_{1,2}$ and the energy spectrum calculation, but for other kind of problems where the full wave functions are necessary (e.g., the calculation of optical transition matrix elements) these corrections may be important.

IV. DISCUSSION

The dependence of the coupling strengths $X_{1,2}$, Eq. (3.6), on the in-plane wave vector $k_\parallel$ can be reduced to dimesionless functions $f_{1,2}$ as follows:

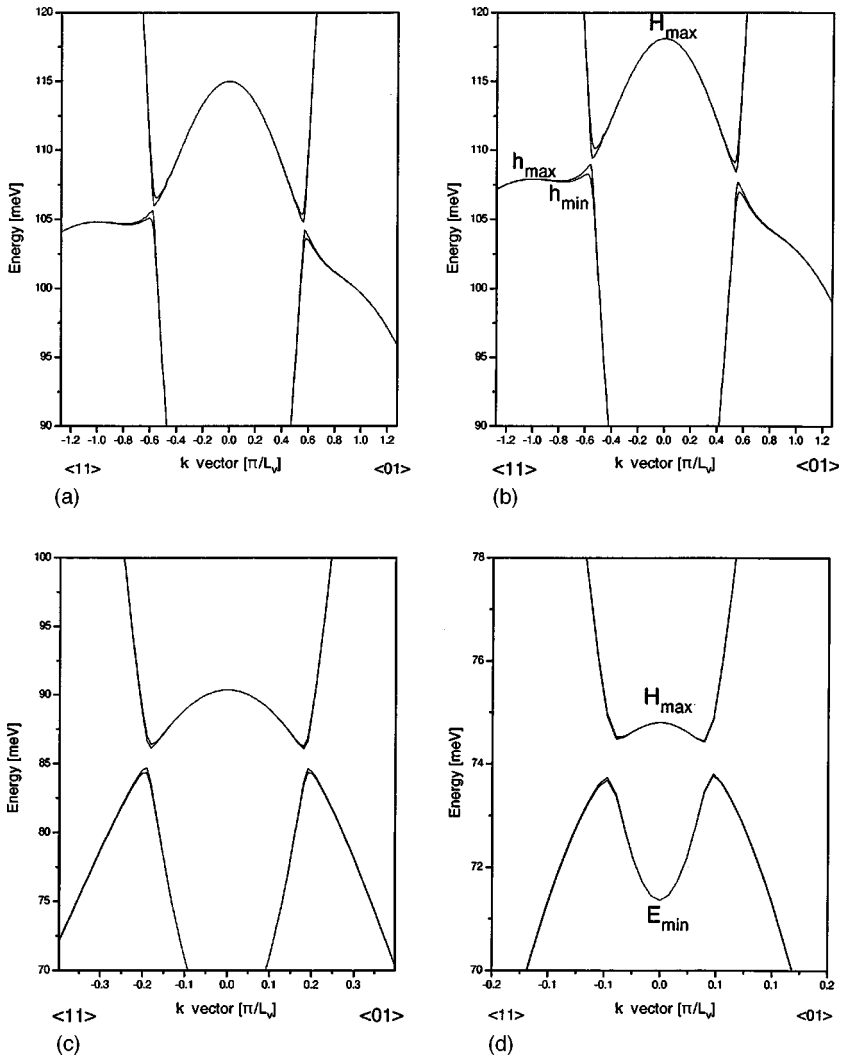

FIG. 3. The energy spectrum for different wells widths including the correction which is induced by the self consistant potential. (a) $L_v=100$ Å, $L_c=170$ Å, (b) $L_v=100$ Å, $L_c=150$ Å, $H_{\max}$ is the top of the first valence sub-band, $h_{\max}$, $h_{\min}$ are, respectively, additional local maximum and minimum of the valence sub-band, in the $\langle 11\rangle$ direction. (c) $L_v=50$ Å, $L_c=150$ Å, (d) $L_v=40$ Å, $L_c=140$ Å. $H_{\max}$ is the top of the first valence sub-band, $E_{\min}$ is the bottom of the first conduction sub-band.

$$X_{1,2}=\left(\frac{\hbar^2 a}{2\sqrt{m_e m_{lh}}}\right)^2 \frac{2\pi^5}{L_c^3 L_v^3} f_{1,2}(k_\parallel L_v). \tag{4.1}$$

The prefactor in this equation gives the energy scale of the coupling. The functions $f_{1,2}$ are shown in Fig. 1. As one can see the coupling strengths are nonmonotonic functions of $k_\parallel$. When $k_\parallel$ goes to zero the coupling strengths also go to zero. To understand this one has to remember that $X_{1,2}$ describe the coupling between the electron ground subband and the heavy hole ground subband. On the other hand electrons are directly coupled to light holes only.[39] The coupling between electrons and heavy holes comes from an admixture of the light hole component to the heavy holes. This admixture goes to zero with $k_\parallel$.

The coupling strength X_2 may also have a zero of another kind, i.e., occasional zero. It happens when the quantity d, Eq. (3.7b), reaches a zero different from $k_\parallel=0$.

In Fig. 2 we present the results of the complete calculation of the band structure for different well widths. From the results that are presented in Fig. 2 we see an important effect of the spectrum anisotropy and of the dependence of the coupling on the in-plane vector. The energy gap induced by the coupling between electrons and holes is located in different places for different crystallographic directions. Since the size of the gap is a function of the in-plane vector, different positions of the gap, yields different gap widths. The hole energy decreases faster with the in-plane vector at the $\langle 01\rangle$ direction. Due to that, the crossing point in the $\langle 01\rangle$ direction is located at smaller in-plane vectors than the crossing point in the $\langle 11\rangle$ direction.

When the wells are narrow [Figs. 2(c),2(d)], the different positions of the crossing points lead to a larger coupling strength at the $\langle 11\rangle$ direction, which yields larger gap and a more pronounced level spliting at this direction. When the wells width is large enough [Figs. 2(a),2(b)] the overlap of the ground sub-bands of InAs electrons and GaSb holes is bigger and the anisotropy effects are even more prominent. Because of the anisotropy the gap arising from the coupling has different energy positions in different directions of the in-plane wave vector. If this difference is larger than the gap itself a new kind of gapless state comes about. The specifics of this situation is that the presence of the gap can be seen in

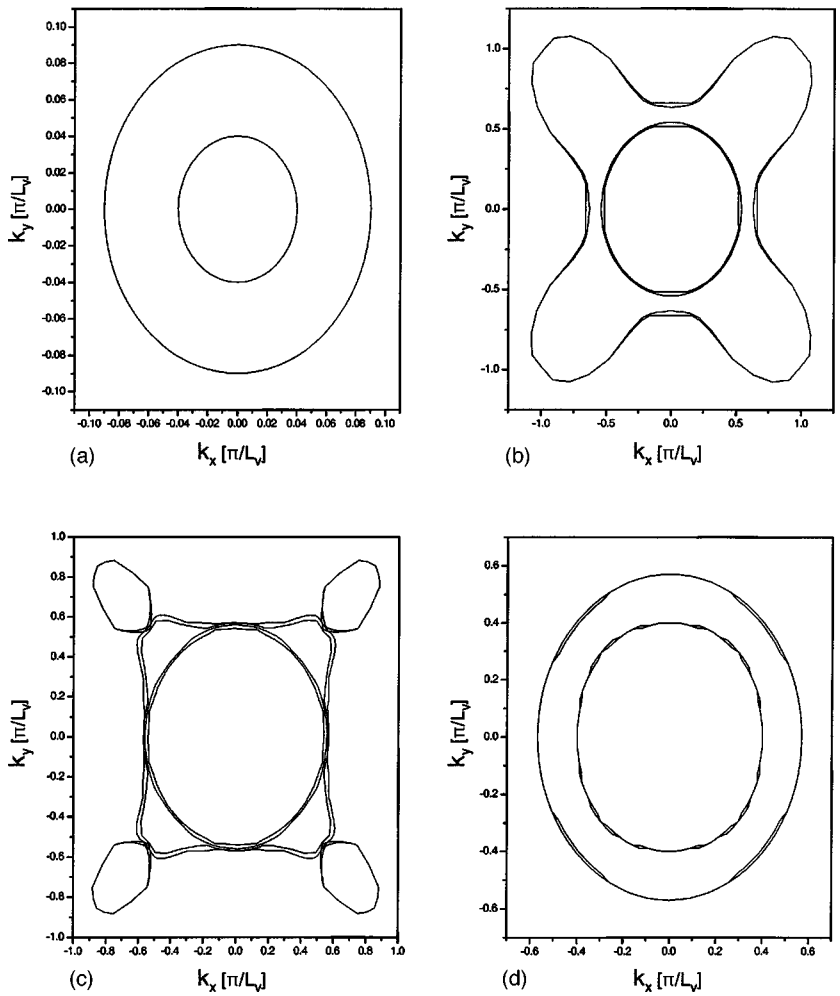

FIG. 4. Various constant energy contours for different wells widths, including the self-consistent potential correction. The zero energy point is taken to be at the bottom of the bulk InAs conduction band. (a) $L_v=40$ Å, $L_c=140$ Å, $E=73$ meV. (b) $L_v=100$ Å, $L_c=150$ Å, $E=106$ meV, (c) $L_v=100$ Å, $L_c=150$ Å, $E=107.5$ meV, (d) $L_v=100$ Å, $L_c=150$ Å, $E=112$ meV.

optical experiments but in the density of states and hence, in transport, the gap does not exist. This may be the explanation of the fact that the first experiment where the gap has been detected[13] was carried out on relatively thin quantum wells [the width of the InAs layer $L_c=140$ Å and the width of the GaSb layer $L_v=40$ Å, Fig. 2(d)]. Without anisotropy two edges of the gap form circles in the k space and the density of states has square root singularities at the edges.[36] An anisotropy breaks the circles and creates saddle points near the edges that smears the singularities to logarithmic ones. If the Fermi level is swept across the gap, the existence of the gap leads to a dip in the conductivity. The density of state singularities lead to an increase of the conductivity near the dip. The weakening of the singularities by the anisotropy makes this increase very weak.[13]

Another important result of the anisotropy is an additional maximum in the hole spectrum in the $\langle 11\rangle$ direction that becomes important in wide enough wells. Due to this maximum constant energy contours in some region of energies become quite nontrivial.

In the actual system there is a self-consistent potential which is induced by charge transfer between the wells. In order to see its effects on the sub-bands and bring our results closer to the experimental situation, we used a simple model that was described in our previous work.[36] In Fig. 3 we present the results of the calculation including the correction of self-consistent potential according to this simple model. Due to the self-consistent potential the electron and the hole sub-bands were shifted towards each other, and the crossing point position moved to lower in-plane vectors. This reduces the anisotropy effect, but all the main features of the spectrum without the correction still hold, including the gapless phase [Figs. 3(a),3(b)].

In Fig. 2(a) one can see a principal possibility of another kind of gapless state. Such a gapless state can arise if the occasional zero of X_2 mentioned above occurs precisely at the crossing point of $E_e^{(0)}$ and $E_h^{(0)}$. This occasional degeneracy can be removed by a change of the system parameters. For example, as one can see from comparison of Fig. 2(a) and Fig. 3(a) that for chosen parameters of the quantum wells it is removed by the self-consistent potential.

In Fig. 4 we present constant energy contours that give cyclotron orbits in the semiclassical approximation.[24,25,40,41] We provide the results that include the self-consistent potential correction, the results without correction will have similar properties.

Here again there is a difference between the results for narrow wells, and for wide wells. First, we will examine the

narrow wells case, e.g., $L_c=140$ Å, $L_v=40$ Å, Fig. 3(d). When the Fermi level is above $H_{\max}$, we will have only an electron orbit. When the Fermi level is between $H_{\max}$ and the gap, we will have one electrons orbit and one hole orbit. In the gap there are no cyclotron orbits. Once we are below the gap but above $E_{\min}$, again we will have two kinds of orbits, electron orbits and hole ones. An example is on Fig. 4(a) for energy equals 73 meV. When the Fermi energy is below $E_{\min}$ we will have only hole orbits. Since the hole spectrum is nonparabolic, for different positions of the Fermi level we will get different values of the hole CR mass, but for each energy position we will get at most two lines in CR experiment, one for holes, and one for electrons.

The situation is different in wider wells, e.g., for the spectrum that is described in Fig. 3(b) ($L_v=100$ Å, $L_c=150$ Å). Here we see that complicated band structure results in different nontrivial constant energy contours, i.e., in a number of cyclotron orbits. The shape of the contours changes substantially within a very small energy interval. The difference between Figs. 4(b), 4(c), and 4(d), is only a few meV. These shapes result from the anisotropy and nonparabolicity of the sub-band structure and could not be obtained from the parabolic approximation. These shapes show that the number of lines in CR experiments can change substantially with a slight change of the Fermi level position. The description of possible orbits above the gaps is the same as for the narrow wells and an example we see in Fig. 4(d) where the energy equals 112 meV. Since this system is gapless, we always have constant energy contours. The contours shapes vary drastically with the change of the Fermi level position within small region near $h_{\min}$, $h_{\max}$. When the energy is between $h_{\max}$ and $h_{\min}$ a typical energy contour has the shape of Fig. 4(c) (107.5 meV). Since we are very close to the crossing point, the splitting of the degenerate subbands is well pronounced and this is why we see the double contours in Figs. 4(b)–4(d). Here we can expect one electron effective mass corresponding to the internal closed contour and at least two different hole effective masses, one corresponding to the central closed contour around Γ_8 point and the other that corresponds to 4 closed contours around the $\langle 11\rangle$ extrema. Any external distortion in some in-plane direction will break the symmetry between the $\langle 11\rangle$ contours and can lead to a larger number of different effective masses for holes. This can explain additional lines in the CR experiments.[42] When the Fermi level is below $h_{\min}$ we have Fig. 4(b) (106 meV) where again we have only two orbits.

V. SUMMARY

In this paper we calculated the energy spectrum of InAs/GaSb heterostructures considering the exact valence band structure. We treated the coupling as a small perturbation for the problem of two decoupled infinite quantum wells, one for holes, and one for electrons. The main results are the existence of a gapless state due to the anisotropy and nontrivial constant energy contours, which might illuminate the CR's fascinating results. The coupling between the layers lifts the degeneracy of the electron and hole ground states and at the crossing point we expect an additional splitting of the energy bands.

APPENDIX: THE DETERMINANT COEFFICIENTS

The notations that we used for the determinant in the second section Eq. (2.14) are the following:

$$C_{21}=\frac{\hbar^2}{2m_0}\frac{\hbar^2}{2m_e}\frac{\mathcal{B}_{21}(\gamma_1+2\gamma_2)}{\mathcal{A}_{h,22}\mathcal{A}_{e,11}-|\mathcal{B}_{21}|^2},\quad C_{32}=\frac{\hbar^2}{2m_0}\frac{\hbar^2}{2m_e}\frac{\mathcal{B}_{32}(\gamma_1+2\gamma_2)}{\mathcal{A}_{h,33}\mathcal{A}_{e,22}-|\mathcal{B}_{32}|^2}, \tag{A1a}$$

$$C_{\uparrow}=\left(\frac{\hbar^2}{2m_e}\right)^2\frac{\mathcal{A}_{h,22}}{\mathcal{A}_{h,22}\mathcal{A}_{e,11}-|\mathcal{B}_{21}|^2},\quad C_{\downarrow}=\left(\frac{\hbar^2}{2m_e}\right)^2\frac{\mathcal{A}_{h,33}}{\mathcal{A}_{h,33}\mathcal{A}_{e,22}-|\mathcal{B}_{32}|^2}, \tag{A1b}$$

$$\begin{aligned}G\left(\left|\frac{\partial\psi_h^{(0)}}{\partial z}\right|^2\right)=&\left[\frac{\hbar^2}{2m_0}(\gamma_1-2\gamma_2)\right]^2\left(\frac{1}{\mathcal{A}_{h,11}}\left|\frac{\partial\tilde{\psi}_{h,3/2}^{(0)}}{\partial z}\right|^2+\frac{1}{\mathcal{A}_{h,44}}\left|\frac{\partial\tilde{\psi}_{h,-3/2}^{(0)}}{\partial z}\right|^2\right)\\&+\left[\frac{\hbar^2}{2m_0}(\gamma_1+2\gamma_2)\right]^2\left(\frac{\mathcal{A}_{e,11}}{\mathcal{A}_{h,22}\mathcal{A}_{e,11}-|\mathcal{B}_{21}|^2}\left|\frac{\partial\tilde{\psi}_{h,1/2}^{(0)}}{\partial z}\right|^2+\frac{\mathcal{A}_{h,33}}{\mathcal{A}_{h,33}\mathcal{A}_{e,22}-|\mathcal{B}_{32}|^2}\left|\frac{\partial\tilde{\psi}_{h,-1/2}^{(0)}}{\partial z}\right|^2\right),\end{aligned} \tag{A1c}$$

$$\begin{aligned}F\left(\frac{\partial\psi_{h,\mathrm{even}}^{*(0)}}{\partial z},\frac{\partial\psi_{h,\mathrm{odd}}^{(0)}}{\partial z}\right)=&-\left[\frac{\hbar^2}{2m_0}(\gamma_1-2\gamma_2)\right]^2\left(\frac{1}{\mathcal{A}_{h,11}}\frac{\partial\tilde{\psi}_{h,\mathrm{even},3/2}^{*(0)}}{\partial z}\frac{\partial\tilde{\psi}_{h,\mathrm{odd},3/2}^{(0)}}{\partial z}+\frac{1}{\mathcal{A}_{h,44}}\frac{\partial\tilde{\psi}_{h,\mathrm{even},-3/2}^{*(0)}}{\partial z}\frac{\partial\tilde{\psi}_{h,\mathrm{odd},-3/2}^{(0)}}{\partial z}\right)\\&+\left[\frac{\hbar^2}{2m_0}(\gamma_1+2\gamma_2)\right]^2\left(\frac{\mathcal{A}_{e,11}}{\mathcal{A}_{h,22}\mathcal{A}_{e,11}-|\mathcal{B}_{21}|^2}\frac{\partial\tilde{\psi}_{h,\mathrm{even},1/2}^{*(0)}}{\partial z}\frac{\partial\tilde{\psi}_{h,\mathrm{odd},1/2}^{(0)}}{\partial z}\right)\\&+\left[\frac{\hbar^2}{2m_0}(\gamma_1+2\gamma_2)\right]^2\left(\frac{\mathcal{A}_{e,22}}{\mathcal{A}_{h,33}\mathcal{A}_{e,22}-|\mathcal{B}_{32}|^2}\frac{\partial\tilde{\psi}_{h,\mathrm{even},-1/2}^{*(0)}}{\partial z}\frac{\partial\tilde{\psi}_{h,\mathrm{odd},-1/2}^{(0)}}{\partial z}\right).\end{aligned} \tag{A1d}$$

The numerical part of the subscripts of the hole wave function denotes the component of the wave function that has this total angular momentum projection in the z direction. Since electron wave functions have only one component that is different than zero [Eq. (2.9)], we did not use numerical subscripts there. Under the assumptions that were described in Sec. II, the only constant that does not vanish is $C_{21}=C_{32}\equiv C$.

[1] Y. Kuramoto and C. Horie, Solid State Commun. **25**, 713 (1978).
[2] S. Datta, M. R. Melloch, and R. L. Gunshor, Phys. Rev. B **32**, 2607 (1985).
[3] L. V. Keldysh, in *Bose-Einstein Condenstion*, edited by A. Griffin, D. W. Snoke, and S. Stringari (Cambridge University Press, New-York, 1994).
[4] I. V. Lerner and Y. E. Lozovik, Solid State Commun. **23**, 43 (1977); J. Phys. C **12**, L501 (1979).
[5] D. Paquet, T. M. Rice, and K. Ueda, Phys. Rev. B **32**, 5208 (1985).
[6] Y. E. Lozovik and V. I. Yudson, JETP Lett. **22**, 274 (1976); Solid State Commun. **19**, 391 (1976).
[7] X. Zhu, J. J. Quinn, and G. Gumbs, Solid State Commun. **75**, 595 (1990).
[8] X. Xia, X. M. Chen, and J. J. Quinn, Phys. Rev. B **46**, 7212 (1991).
[9] Y. Naveh and B. Laikhtman, Phys. Rev. Lett. **77**, 900 (1996).
[10] J.-P. Cheng, J. Kono, B. D. McCombe, I. Lo, W. C. Mitchel, and C. E. Stutz, Phys. Rev. Lett. **74**, 450 (1995).
[11] G. H. Döhler, Surf. Sci. **98**, 108 (1980).
[12] Y. Naveh and B. Laikhtman, Appl. Phys. Lett. **66**, 1980 (1995).
[13] M. J. Yang, C. H. Yang, B. R. Bennett, and B. V. Shanabrook, Phys. Rev. Lett. **78**, 4613 (1997).
[14] R. J. Wagner, B. V. Shanabrook, M. J. Yang, and J. R. Waterman, Superlattices Microstruct. **21**, 95 (1997).
[15] L. J. Cooper, N. K. Patel, V. Drouot, E. H. Linfield, D. A. Ritchie, and M. Pepper, Phys. Rev. B **57**, 11 915 (1998).
[16] M. Lakrimi, S. Khym, R. J. Nicholas, D. M. Symons, F. M. Peeters, N. J. Mason, and P. J. Walker, Phys. Rev. Lett. **79**, 3034 (1997).
[17] D. Heitmann, M. Ziesmann, and L. L. Chang, Phys. Rev. B **34**, 7463 (1986).
[18] M. J. Yang, R. J. Wagner, B. F. Shanabrook, J. R. Waterman, and W. J. Moore, Phys. Rev. B **47**, 6807 (1993).
[19] J. Kono, B. D. McCombe, J.-P. Cheng, I. Lo, W. C. Mitchel, and C. E. Stutz, Phys. Rev. B **50**, 12 242 (1994).
[20] J. Kono, B. D. McCombe, J.-P. Cheng, I. Lo, W. C. Mitchel, and C. E. Stutz, Phys. Rev. B **55**, 1617 (1997).
[21] J. M. Luttinger and W. Kohn, Phys. Rev. **97**, 869 (1955).
[22] S. S. Nedorezov, Sov. Phys. Solid State **12**, 1814 (1971).
[23] A. Matulis and K. Piragas, Fiz. Tekn. Poluprovodn. **9**, 2202 (1975) [Sov. Phys. Semicond. **9**, 2202 (1975)].
[24] A. V. Chaplik and L. D. Shvartsman, Poverkhnost **2**, 73 1982 [Sov. Phys. Surf.: Phys., Chem., Mech. **2**, 73 (1982)].
[25] L. D. Shvartsman, Solid State Commun. **46**, 787 (1983).
[26] L. C. Andreani, A. Pasquarello, and F. Bassani, Phys. Rev. B **36**, 5887 (1987).
[27] B. Laikhtman, R. A. Kiehl, and D. J. Frank, J. Appl. Phys. **70**, 1531 (1991).
[28] G. A. Sai-Halasz, R. Tsu, and L. Esaki, Appl. Phys. Lett. **30**, 651 (1977); G. A. Sai-Halasz, L. Esaki, and W. A. Harrison, Phys. Rev. B **18**, 2812 (1978).
[29] M. Altarelli, Phys. Rev. B **28**, 842 (1983).
[30] A. Fasolino and M. Altarelli, Surf. Sci. **142**, 322 (1984).
[31] M. Altarelli, J. C. Maar, L. L. Chang, and L. Esaki, Phys. Rev. B **35**, 9867 (1987).
[32] D. Z. Y. Ting, E. T. Yu, and T. C. McGill, Phys. Rev. B **45**, 3583 (1992).
[33] M. A. Davidovich, E. V. Anda, C. Tejedor, and G. Platero, Phys. Rev. B **47**, 4475 (1993).
[34] Jih-Chen Chiang, Shion-Fon Tsay, Z. M. Chan, and Ikai Lo, Phys. Rev. Lett. **77**, 2053 (1996).
[35] Smadar de-Leon, B. Laikhtman, and L. D. Shvartsman, J. Phys.: Condens. Matter **10**, 8715 (1998).
[36] B. Laikhtman, Smadar de-Leon, and L. D. Shvartsman, Solid State Commun. **104**, 257 (1997).
[37] G. L. Bir and G. E. Pikus, in *Symmetry and Strain-Induced Effects in Semiconductors* (Wiley, New-York, 1974), Sec. 26.
[38] E. L. Ivchenko, A. Y. Kaminski, and U. Rossler, Phys. Rev. B **54**, 5852 (1996).
[39] S. R. White and L. J. Sham, Phys. Rev. Lett. **47**, 879 (1981).
[40] O. V. Kibis and L. D. Shvartsman, Sov. Phys. Surf.: Phys. Chem. Mech. **7**, 119 (1985).
[41] G. Shechter, L. D. Shvartsman, and J. E. Golub, Phys. Rev. B **51**, 10 857 (1995).
[42] R. J. Wagner, B. V. Shanabrook, B. R. Bennett, M. J. Yang, and J. R. Waterman, Bull. Am. Phys. Soc. **41**, 367 (1996).